MECHANICAL LOADING OF NEURONS AND ASTROCYTES WITH APPLICATION TO BLAST TRAUMATIC BRAIN INJURY

Kristin B. Bernick, Thibault P. Prevost, Subra Suresh, Simona Socrate*
Massachusetts Institute of Technology
77 Massachusetts Avenue
Cambridge, MA, 02139

ABSTRACT

Investigations of the mechanical properties of cells are essential for linking mechanical deformation and loading to injury mechanisms at the cellular level. This is especially important when studying traumatic brain injury (TBI). Neurons and astrocytes are susceptible to damage mechanisms arising from various loading scenarios, ranging from motor vehicle accidents to sports injuries and pressure waves generated by explosions. Obtaining the mechanical properties of cells of the central nervous system (CNS) is a critical step for the development of hierarchical models and multi-scale simulation tools to elucidate how applied macroscopic loading conditions, such as pressure waves, translate into cell deformation and damage. Here we present atomic force microscopy (AFM) indentation data and finite element simulation results on the mechanical response of single neurons and astrocytes to dynamic loading at large strains. Specific AFM testing protocols were developed to characterize the mechanical behavior of both cortical neurons and astrocytes over a range of indentation rates spanning three orders of magnitude – *i.e.* 10, 1, and 0.1 μm/s. The response of both cell types showed similar qualitative nonlinear viscoelastic patterns although, quantitatively, some differences were noted between the two CNS cell populations. The rheological data were complemented with geometrical measurements of cell body morphology obtained through bright-field and confocal microscopy images. A constitutive model was developed, enabling quantitative comparisons within and between populations of neurons and astrocytes. The proposed model, built upon previous constitutive model developments carried out at the cortical tissue level, was implemented into a three-dimensional finite element framework. The simulated cell responses were successfully calibrated to the experimental measurements under the selected test conditions. The sets of material parameters extracted via the numerical method for both cell types suggest that astrocytes and neurons exhibit distinct viscoelastic behaviors. The body of experimental measurements and numerical results hereby presented provides a solid, preliminary knowledge base, from which further developments may be pursued to unravel the key mechanical pathways potentially involved in TBI.

1. INTRODUCTION

Traumatic brain injury (TBI) is prominent in the civilian and military populations, affecting approximately 2 million civilians each year in the United States alone (Kraus; McArthur 1996), and an estimated 20% of the veteran population returning from Iraq and Afghanistan (Hoge et al. 2009; Tanielian; Jaycox 2008). While the mild or serve forms of TBI are in most cases the result of well-identified insult events (*e.g.* falls, car accidents, sports encounters, blast exposures), the damage progression and long term health consequences associated with TBI remain poorly understood (Belanger et al. 2009; Corrigan et al. 2010; Crowe et al. 2010; Lew et al. 2005; McCrory et al. 2005; Meehan; Bachur 2009; Taber et al. 2006; Vanderploeg et al. 2007; Yilmaz; Pekdemir 2007). An improved understanding of the mechanisms by which macroscopic loading conditions translate into local cell deformation and damage is warranted to gain better insights into the observed health consequences associated with TBI. An important intermediate step in the development of multi-scale models to investigate damage mechanisms involved in the cascade of events leading to traumatic brain injury is the quantitative assessment of CNS cell material properties. Many experimental techniques have been developed to measure the mechanical properties of single cells (for a review, see for example (Bao; Suresh 2003; Suresh 2007; Van Vliet et al. 2003); however, there currently exists no substantial body of work – experimental or theoretical – on the material properties of single cells belonging to the central nervous system, *e.g.* neurons and glia. Lu et al. measured and compared the viscoelastic properties of neurons and astrocytes at small deformation in the linear regime (Lu et al. 2006). Their preliminary results suggest that astrocytes are more compliant than neurons at small strains. At large strains however, *i.e.* in a regime of deformation of relevance in TBI cases, no investigation of the dynamic behavior of CNS cells is currently available in the literature. The present study is a partial answer to address these limitations.

2. METHODS

2.1 Cell Culture

Report Documentation Page

Form Approved
OMB No. 0704-0188

1. REPORT DATE	2. REPORT TYPE	3. DATES COVERED
2010		**00-00-2010 to 00-00-2010**

4. TITLE AND SUBTITLE	5a. CONTRACT NUMBER
Mechanical Loading of Neurons and Astrocytes with Application to Blast Traumatic Brain Injury	5b. GRANT NUMBER
	5c. PROGRAM ELEMENT NUMBER
6. AUTHOR(S)	5d. PROJECT NUMBER
	5e. TASK NUMBER
	5f. WORK UNIT NUMBER
7. PERFORMING ORGANIZATION NAME(S) AND ADDRESS(ES) **Massachusetts Institute of Technology,77 Massachusetts Avenue,Cambridge,MA,02139**	8. PERFORMING ORGANIZATION REPORT NUMBER
9. SPONSORING/MONITORING AGENCY NAME(S) AND ADDRESS(ES)	10. SPONSOR/MONITOR'S ACRONYM(S)
	11. SPONSOR/MONITOR'S REPORT NUMBER(S)

12. DISTRIBUTION/AVAILABILITY STATEMENT

Approved for public release; distribution unlimited

13. SUPPLEMENTARY NOTES

To be presented at The 27th Army Science Conference (ASC), sponsored by the Assistant Secretary of the Army (Acquisition, Logistics and Technology), will be held at the JW Marriott Grande Lakes, Orlando, Florida, November 29 - December 2, 2010.

14. ABSTRACT

Investigations of the mechanical properties of cells are essential for linking mechanical deformation and loading to injury mechanisms at the cellular level. This is especially important when studying traumatic brain injury (TBI). Neurons and astrocytes are susceptible to damage mechanisms arising from various loading scenarios ranging from motor vehicle accidents to sports injuries and pressure waves generated by explosions. Obtaining the mechanical properties of cells of the central nervous system (CNS) is a critical step for the development of hierarchical models and multi-scale simulation tools to elucidate how applied macroscopic loading conditions such as pressure waves, translate into cell deformation and damage. Here we present atomic force microscopy (AFM) indentation data and finite element simulation results on the mechanical response of single neurons and astrocytes to dynamic loading at large strains. Specific AFM testing protocols were developed to characterize the mechanical behavior of both cortical neurons and astrocytes over a range of indentation rates spanning three orders of magnitude ? i.e. 10, 1, and 0.1 μm/s. The response of both cell types showed similar qualitative nonlinear viscoelastic patterns although, quantitatively some differences were noted between the two CNS cell populations. The rheological data were complemented with geometrical measurements of cell body morphology obtained through bright-field and confocal microscopy images. A constitutive model was developed, enabling quantitative comparisons within and between populations of neurons and astrocytes. The proposed model, built upon previous constitutive model developments carried out at the cortical tissue level, was implemented into a three-dimensional finite element framework. The simulated cell responses were successfully calibrated to the experimental measurements under the selected test conditions. The sets of material parameters extracted via the numerical method for both cell types suggest that astrocytes and neurons exhibit distinct viscoelastic behaviors. The body of experimental measurements and numerical results hereby presented provides a solid preliminary knowledge base, from which further developments may be pursued to unravel the key mechanical pathways potentially involved in TBI.

15. SUBJECT TERMS

16. SECURITY CLASSIFICATION OF:			17. LIMITATION OF ABSTRACT	18. NUMBER OF PAGES	19a. NAME OF RESPONSIBLE PERSON
a. REPORT	b. ABSTRACT	c. THIS PAGE			
unclassified	**unclassified**	**unclassified**	**Same as Report (SAR)**	**8**	

Neurons and astrocytes were obtained from cortices of postnatal day 1 Sprague-Dawley rats (Charles River Laboratories, Wilmington, MA), following a protocol approved by the Committee on Animal Care at the Massachusetts Institute of Technology. Cell suspensions were obtained via dissociation in an enzyme solution (1 mM L-cysteine, 0.5 mM EDTA, 1.5 mM $CaCl_2$, 200 units Papain (Sigma, P3125), and 1 µg/mL DNase (Sigma) in 10 mL modified HBSS) followed by mechanical trituration in culture media as previously described in further detail (Bernick et al, 2010). For neuronal cultures, the resulting cell suspension was plated on poly-D-lysine (Sigma, P7886) coated 35 mm, round coverslips (Carolina Biological Supply, Burlington, NC) in Neurobasal media supplemented with B27 and Glutamax (Invitrogen, 21103049, 17504044, 35050061). Neurons were allowed to grow in culture for 5 days prior to testing, *i.e.* until they had well-developed processes. For astrocytic cultures, the cell suspension was plated in culture flasks in Neurobasal medium supplemented with B27, Glutamax, and 10 % fetal bovine serum. Astrocyte cultures were grown to confluence and passaged onto 35 mm PDL coated coverslips 1 day prior to AFM testing. For both neuronal and astrocytic cultures, half of the medium was changed every 3-4 days.

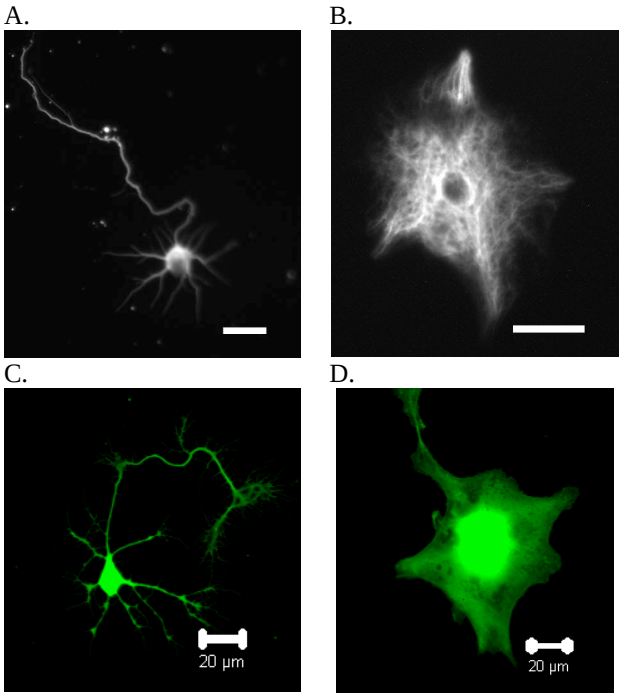

Figure 1: Immunocytochemistry verifying neuronal cell growth in serum free medium (A) and astrocyte growth in serum containing medium (B). Neuron (C) and astrocyte (D) stained with calcein-AM to verify cell viability at time of AFM testing. All scale bars are 20 µm.

Cell type was verified via immunocytochemistry. Anti-β-III tubulin (Abcam, ab24629) and anti-glial fibrillary acidic protein (GFAP) (Abcam, ab4648) were used to identify neurons and astrocytes, respectively (Figures 1A and 1B). Cells grown in serum free medium were shown to be primarily neurons while those grown in serum containing medium were found to be primarily astrocytes. Cell viability at the time of testing was determined using a Live/Dead cytotoxicity assay (Invitrogen, L-3224) (Figures 1C and 1D). In the course of the AFM experiments, cell type was determined based on cell morphology as observed through the bright-field microscope.

2.2 AFM Experiments

Cell properties were determined with an atomic force microscope (MFP 3D, Asylum Research, Santa Barbara, CA) mounted either on an inverted optical microscope for neuron tests (Axio Observer.D1, Carl Zeiss MicroImaging Inc, Thornwood, NY) or on a confocal microscope for astrocyte tests (LSM 700, Carl Zeiss MicroImaging Inc, Thornwood, NY). The AFM probes used were tipless, triangular shaped silicon nitride cantilevers (Veeco Probes NP-OW, 0.06 N/m; Nanoworld PNP-TR-TL, 0.08 N/m) modified with polystyrene spheres (45 µm diameter, Polybead® Microspheres; Polysciences Inc, Warrington, PA). The microspheres were chosen to be large relative to the size of the cellular components in order to enable the probing of global mechanical properties (as opposed to local properties probed by sharp tips (Lulevich et al. 2006)). The microspheres were glued to the end of the silicon nitride probes using UV curable Loctite 3211 and they were cured for 1 h under UV light. Scanning electron microscopy was used to validate the size and positioning of the bead for one representative tip (Figure 2A).

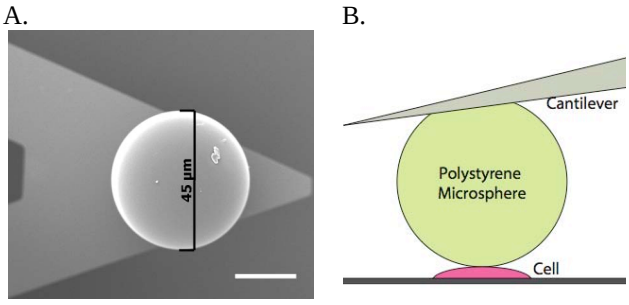

Figure 2: (A) SEM image of one representative cantilever modified with a 45 µm sphere; scale bar is 20 µm. (B) Schematic of AFM experimental set-up.

All tests were conducted at 37 °C in culture medium in a fluid cell chamber (BioHeater™, Asylum Research, Santa Barbara, CA). Tests lasted less than 2 h, and cells remained healthy and viable throughout the duration of the experiment, as determined through visual inspection through a bright-field microscope. Prior to testing, the AFM cantilever was lowered into the medium and allowed to equilibrate for 30 min. Calibration of the spring constant was achieved for each cantilever using the

thermal method built into the AFM software (Matei et al. 2006). Either the somata of neurons or the region of astrocytes located directly above the nucleus were indented during the experiment, as shown schematically in Figure 2B.

A.

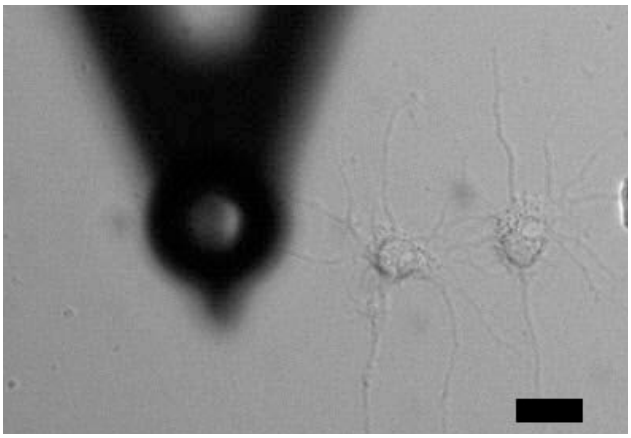

B.

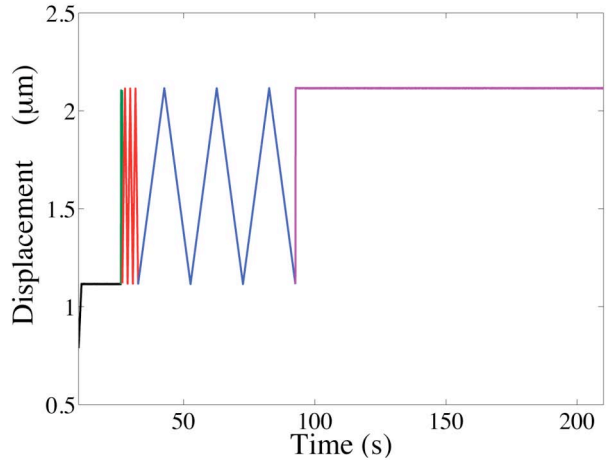

Figure 3: (A) Bright-field microscopy image of AFM cantilever and microsphere adjacent to neuron to be indented; scale bar is 20 μm. (B) AFM loading procedure for astrocytes including approach (black), 10 μm/s (green), 1 μm/s (red), and 0.1 μm/s (blue) loading rates, and stress relaxation (magenta).

All tests were conducted with the aid of light microscopy, *i.e.* bright-field optical microscopy for both neurons and astrocytes and additional epi-fluorescence/ confocal microscopy for astrocytes. The latter observation technique enabled more accurate positioning of the AFM probe relative to the astrocyte nucleus, thereby yielding more precise sets of geometrical measurements. A typical bright-field image of a neuron experiment is shown in Figure 3A where the neuron to be indented is captured adjacent to the AFM cantilever. The center of either the neuron cell body or the astrocyte nucleus was aligned with the vertical Z-axis of the indenting sphere through the 20X magnification objective. The indentation test sequence, implemented as a custom routine in IGOR Pro software (WaveMetrics, Inc, Portland, OR), consisted of an approach phase at 0.3 μm/s to a 0.3 nN target force followed by a 15 s dwell phase during which the cell-probe system was allowed to equilibrate, and a subsequent series of load–unload segments at 10, 1, and 0.1 μm/s followed by a 120 s relaxation test. Neurons were indented to 2 μm indentation depth and astrocytes to only 1 μm due to their more flattened, spread conformation. The loading sequence applied to astrocytes is shown in Figure 3B. The loading rates were selected to span the broadest range of deformation speeds compatible with the MFP 3D capabilities and the physical limitations pertaining to the test configuration.

2.3 Cell Geometry Measurements

For neuron measurements, cell height was determined after the indentation tests, following a procedure adapted from other AFM height determination methods (Lulevich et al. 2006; Spagnoli et al. 2007). Briefly, additional indentation tests were performed on the cell body and at 2-3 positions on the adjacent glass substrate at a speed of 10 μm/s to a target force of 4.5 nN. The piezo position at contact with either cell or glass was determined. The difference in positions between the cell- and glass-cantilever contact events was taken as the cell height. The glass–cantilever contact point was determined from the intersection between the pre- and post-contact linear fit to the measured force curve. Due to the soft nature of the cells, the cell–cantilever contact point was determined using a hierarchical Bayesian approach described in detail in section 6.1 of (Rudoy et al. 2010). All contact point and height calculations were performed in MATLAB (The MathWorks, Inc.). Average neuron cross-sectional diameter was obtained from the bright field microscopy images taken for each cell.

For astrocyte studies, a confocal microscope (LSM 700, Carl Zeiss MicroImaging Inc, Thornwood, NY) was coupled with the AFM. Astrocytes were loaded with 2 μM calcein-AM (cytoplasmic stain) and 1.6 μM Hoechst 33342 (nuclear stain) in PBS at 37 °C for 15 min. Following dye-loading, cells were returned to culture medium and allowed to recover in the incubator at 37 °C for 45 min prior to loading on the AFM. Epifluorescence was used to determine and adjust the position of the AFM tip relative to that of the cell nucleus. This step was deemed necessary to ensure consistency with the neuron measurements, which were performed on the cell body, *i.e.* above the nucleus. Confocal Z-stacks were taken following indentation to obtain the gross 3D structure of the cell. The resulting images were used to determine cross-sectional diameter and height. Images for a representative astrocyte are shown in Figure 4. The cytoplasm is shown in green, the cell nucleus in pale blue, and the AFM probe in deeper blue. The top and side

views show the AFM probe position relative to the nucleus.

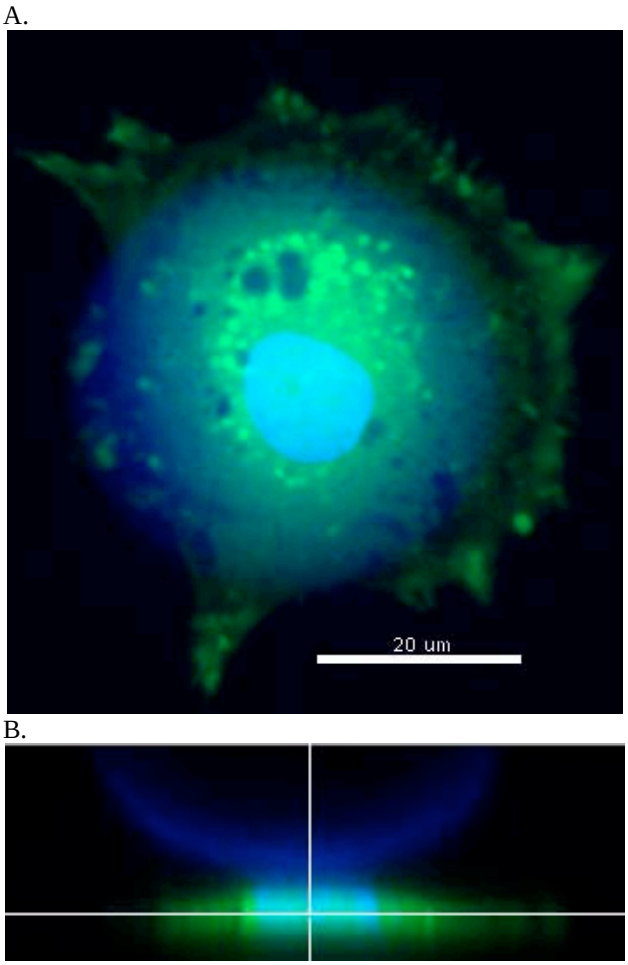

Figure 4: Fluorescence image showing positioning of AFM probe above astrocyte nucleus (top and side view). The cytoplasm is shown in green (calcein-AM), the nucleus in pale blue (Hoechst 33342), and the AFM probe microsphere in deeper blue.

To control for discrepancies between the two height determination methods applied to neurons and astrocytes, both methods were implemented on a small population of neurons. The AFM determination method was applied first, followed by acquisition of a confocal Z-stack.

2.4 Finite Element Simulations

The AFM data sets obtained on neurons and astrocytes were analyzed using finite element modeling in ABAQUS through a user defined material model. The cell geometry was taken to be an oblate spheroid whose cross-diameter and height were defined for each cell based on the corresponding experimental measurements. The AFM tip was modeled as a rigid spherical indenter (Figure 5A).

Building upon the similarities in mechanical response observed at the cell and tissue levels, we selected a material model for the cell directly adapted from the model previously developed to characterize the dynamic behavior of porcine cortices (Prevost et al. 2010). The model formulation is described in depth in (Prevost et al. 2010) and (Bernick et al. 2010). Briefly, it comprises a hyperelastic network accounting for the instantaneous cell response and four viscoelastic components capturing the strain rate effects at both short and long time scales (Figure 5B). The model requires eight material parameters. *K* represents the small strain bulk modulus, (μ_o, λ_L) mediate the instantaneous (elastic) response of the cell in shear, and (σ_o, n) and (G_o, G_∞, η) address the time-dependencies at short and long time scales, respectively. For specific details on the constitutive equations the reader is referred to (Prevost et al. 2010).

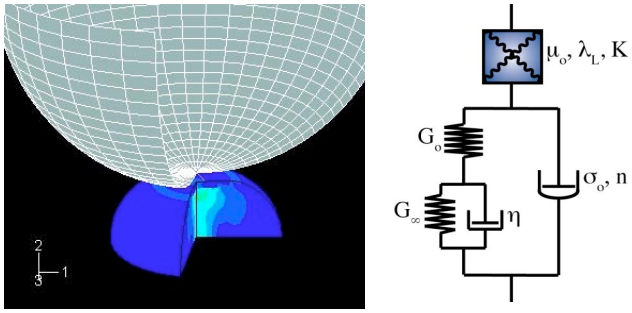

Figure 5: (A) ABAQUS geometry used for neuron simulations. (B) Schematic of rheological model and parameters used to simulate cell behavior.

The full experimental loading sequence was simulated using ABAQUS and the parameters were varied to optimize the fit of the model to the AFM data. Both average AFM data and single cell data were used for fitting, and the model geometry was modified to match that of either average dimensions or single cell measurements.

3. RESULTS

The mechanical response of neurons and astrocytes to AFM indentation exhibited non-linearities, hysteresis, rate-dependencies and conditioning. Figure 6 shows a representative set of force versus time and force versus displacement measurements for a single neuron (6A and 6C) and for a single astrocyte (6B and 6D).

To ensure that the presence of dye in the medium did not alter the measured material properties of astrocytes, additional tests were performed as a control in the absence of dye. As shown in Figure 7, the cell response was found to be indifferent to the loading of dye.

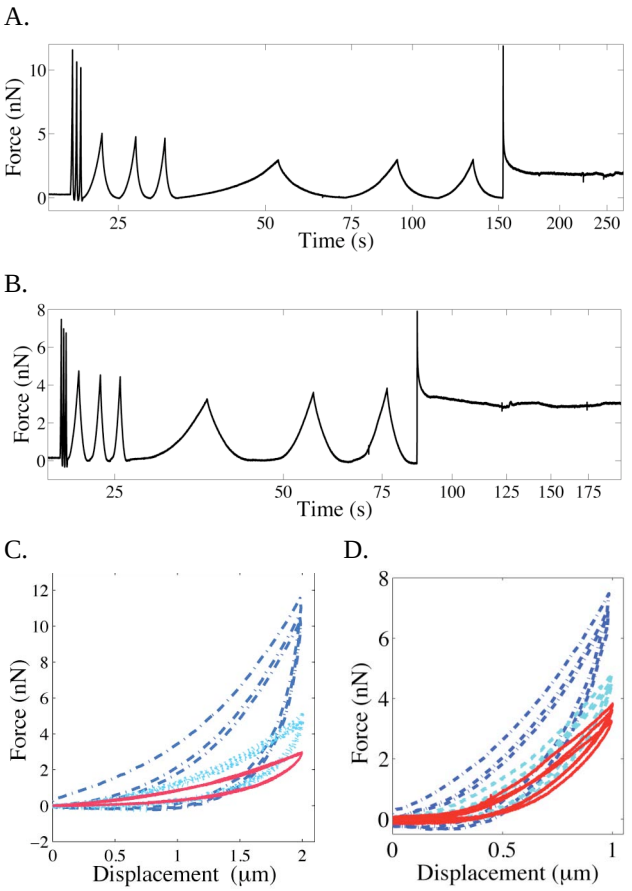

Figure 6: Representative force vs. time/displacement curves for a single neuron (A)/(C) and an astrocyte (B)/(D) (10 μm/s = blue dash, 1 μm/s = cyan dash, 0.1 μm/s = red line).

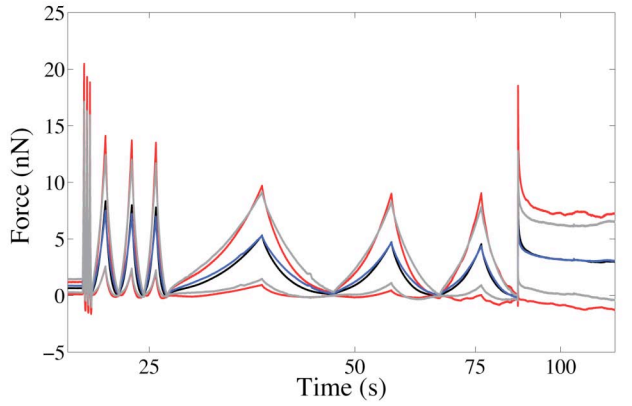

Figure 7: Dye-loaded astrocytes (n = 37; Mean = black; +/- standard deviation = red) compared with unloaded astrocytes (n = 9; Mean = blue; +/- standard deviation = grey)

Although all cells were shown to follow similar trends to those depicted in Figure 6, significant variations in cell height and radius were observed. In the neuron case, height measurements were found to range between 4.5 and 14 μm, with a mean of 7.9 μm, whereas radius estimates fell between 6.2 and 11.5 μm, with a mean of 8.4 μm. Astrocytes were found to be thinner and larger than neurons with a representative astrocyte cell selected for initial modeling having a height of 5 μm and a radius of 18 μm. The two height determination methods, via AFM and confocal imaging respectively, were shown to yield comparable results (Table 1).

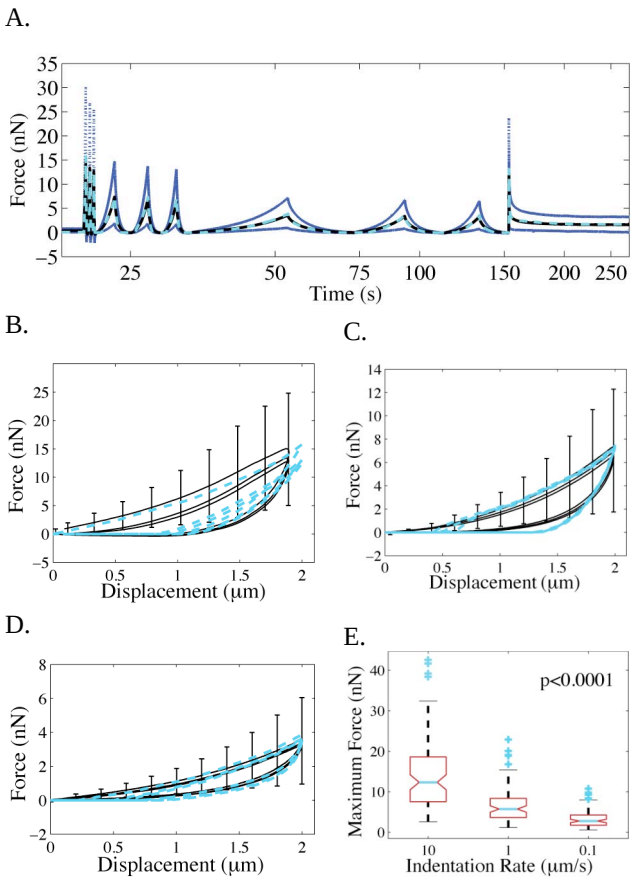

Figure 8: Mean AFM response for neurons (n = 87) and model fit using set of parameters shown in Table 2. (A) Force vs time responses measured (average, black; +/- standard deviation, blue) and simulated (cyan dash). (B, C, D) Force vs displacement responses at 10 μm/s, 1 μm/s, and 0.1 μm/s, measured (average with standard deviations, black) and simulated (cyan dash). (E) Peak forces reached at each loading rate. Rate effects were statistically significant (ANOVA, $p < 0.0001$).

The model was fit to a selected set of AFM mechanical data collected on neurons and astrocytes. In the neuron case, the response was fit to the average set of force-displacement measurements (n = 87) as shown in Figure 8. The model cell employed in the numerical simulations was taken to have a radius of 8.5 μm and a height of 8 μm, *i.e.* dimensions matching the average measured values. In the astrocyte case, the response was

fit to a representative set of measurements (Figure 9). The model dimensions were taken to match those of the actual representative cell (radius = 18 μm; height = 5 μm). The optimized material parameters obtained for each cell type are listed in Table 2. The proposed model was able to accurately capture all aspects of the cell responses, in load-unload at all 3 loading rates as well as in relaxation.

Neuron	Height from AFM (μm)	Height from Confocal (μm)
1	9.85	9.93
2	8.39	8.32
3	9.95	9.89
4	7.10	7.12
5	7.48	7.56
Mean	8.55	8.56
Standard Deviation	1.32	1.30

Table 1: Comparison between height measurements obtained on 5 representative neurons using both the AFM height determination method and the confocal imaging method.

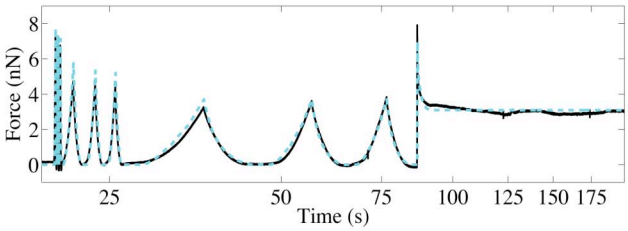

Figure 9: Representative AFM response (black) for single astrocyte and model fit (cyan dash) using set of parameters shown in Table 2.

Parameter	Neuron (Mean Response; n=87)	Astrocyte (Single Cell Response)
G_o (Pa)	75	520
n	1	0.85
σ_o (Pa)	0.005	0.0032
λ_L	1.05	1.09
μ_o (Pa)	16	13.9
η (Pa.s)	3000	440
G_∞ (Pa)	40	130

Table 2: Model parameters obtained by fitting mean AFM data for neurons (n = 87) and a representative set of single astrocyte measurements.

4. DISCUSSION

The dynamic responses of neurons and astrocytes showed similar qualitative trends (*e.g.* hysteretic features, time dependencies, nonlinearities) while exhibiting some notable quantitative differences. Astrocyte responses (Figure 9) were found to be less rate-dependent than neuron responses (Figure 8A) where the AFM force for the low-rate cycles is more significantly reduced for the neuron population, and the equilibrium response in relaxation is much lower than the peak force. This is reflected by differences between the optimized material parameter values shown in Table 2, where the ratios of viscoelastic to instantaneous moduli (G_o/μ_o and G_∞/μ_o) were found to be significantly higher for astrocytes. To our knowledge, this is the first time this trend has been reported in quantifiable terms. In the work by Lu et al. focusing on the small strain behavior of neural cells such differences in viscous effects were not noted, suggesting that these latter differences might more specifically pertain to the large deformation regime. At small deformations, Lu et al. reported astrocytes to be more compliant than neurons with pseudo Young moduli E' ranging between 480 Pa at 30 Hz and 970 Pa at 200 Hz for neurons and between 300 Pa at 30 Hz and 520 Pa at 200 Hz for astrocytes. These results are corroborated by those obtained in the present study where similar softening trends were noted for astrocytes at small strains – as attested by the optimized parameter values found for λ_L and μ_o. μ_o (proportional to cell "stiffness") and λ_L (inversely proportional to "stiffness") were found to be respectively 13.9 Pa and 1.09 for astrocytes as opposed to 16 Pa and 1.05 for neurons.

As evidenced by the large standard deviations shown in Figures 7 and 8, the AFM mechanical measurements obtained for both astrocytes and neurons were marked by substantial variations. Differences in geometrical features are likely to account for some of these observed variations in cell response. Other potential sources of variability include differences in cell types (*e.g.* excitatory vs inhibitory neurons), stages in cell cycle (astrocytes are actively dividing in culture), and initial location of cell-cantilever contact. Some of these sources of variation will be further investigated in future studies in order to decrease the scatter in the data.

The work presented here provides the first substantial quantitative set of mechanical measurements conducted at large strains on single neurons and astrocytes. The constitutive model proposed in support of these observations represents a critical first step towards the development of multi-scale models that may be used to study and simulate the effects of macroscopic mechanical transients on the local cell environment.

5. CONCLUSIONS

The present study uncovers novel features pertaining to the large strain dynamic mechanical behavior of single neurons and astrocytes. The key cell response features (*e.g.* nonlinearities, hysteresis, and time dependencies) were measured and contrasted at loading rates spanning three orders of magnitude. The constitutive model

developed to account for the neural cell behaviors was able to accurately capture the main characteristics of the cell responses. The data collected and the constitutive framework proposed may crucially help expand our knowledge of individual CNS cell responses to mechanical trauma.

ACKNOWLEGDEMENTS

This work was supported by the US Army Research Office and Joint Improvised Explosive Devices Defeat Organization, under contract number W911NF-07-1-0035; the MIT Institute for Soldier Nanotechnologies, under contract number W911NF-07-D-0004; the National Science Foundation Graduate Research Fellowship Program; the National Institutes of Health Molecular, Cell, and Tissue Biomechanics Training Grant; and École Nationale des Ponts et Chaussées (Université Paris-Est, France). Partial support was also provided by the Computational Systems Biology Programme of the Singapore-MIT Alliance (SMA) and the Interdisciplinary Research Group on Infectious Diseases at the Singapore-MIT Alliance for Research and Technology (SMART). The authors are grateful to Professor Sebastian Seung (Massachusetts Institute of Technology, Cambridge, USA) for providing cortical tissue, Professor Patricia Carvalho (Instituto Superior Técnico, Lisbon, Portugal) for imaging SEM samples, and Dr. Shelten Yuen and Daniel Rudoy (Harvard University, Cambridge, USA) for providing the MATLAB routine employed in the determination of the cell-cantilever contact point.

REFERENCES

Bao, G., and S. Suresh, 2003: Cell and molecular mechanics of biological materials. *Nature Materials*, **2,** 715-725.

Belanger, H. G., T. Kretzmer, R. Yoash-Gantz, T. Pickett, and L. A. Tupler, 2009: Cognitive sequelae of blast-related versus other mechanisms of brain trauma. *J. Int. Neuropsychol. Soc.*, **15,** 1-8.

Bernick, K. B., T. P. Prevost, S. Suresh, and S. Socrate, 2010: Biomechanics of Single Cortical Neurons. *Acta Biomaterialia*, **in review**.

Corrigan, J. D., A. W. Selassie, and J. A. L. Orman, 2010: The epidemiology of traumatic brain injury. *J Head Trauma Rehabil*, **25,** 72-80.

Crowe, L. M., V. Anderson, C. Catroppa, and F. E. Babl, 2010: Head injuries related to sports and recreation activities in school-age children and adolescents: Data from a referral centre in Victoria, Australia. *Emergency Medicine Australasia*, **22,** 56-61.

Hoge, C., H. Goldberg, and C. Castro, 2009: Care of War Veterans with Mild Traumatic Brain Injury--Flawed Perspectives. *The New England Journal of Medicine*, **360,** 1588.

Kraus, J. F., and D. L. McArthur, 1996: Epidemiologic aspects of brain injury. *Neurologic Clinics*, **14,** 435.

Lew, H. L., J. H. Poole, S. Alvarez, and W. Moore, 2005: Soldiers with occult traumatic brain injury. *American Journal of Physical Medicine & Rehabilitation*, **84,** 393-398.

Lu, Y. B., and Coauthors, 2006: Viscoelastic properties of individual glial cells and neurons in the CNS. *Proceedings of the National Academy of Sciences of the United States of America*, **103,** 17759-17764.

Lulevich, V., T. Zink, H. Y. Chen, F. T. Liu, and G. Y. Liu, 2006: Cell mechanics using atomic force microscopy-based single-cell compression. *Langmuir*, **22,** 8151-8155.

Matei, G. A., E. J. Thoreson, J. R. Pratt, D. B. Newell, and N. A. Burnham, 2006: Precision and accuracy of thermal calibration of atomic force microscopy cantilevers. *Review of Scientific Instruments*, **77**.

McCrory, P., M. Makdissi, G. Davis, and A. Collie, 2005: Value of neuropsychological testing after head injuries in football. *British Journal of Sports Medicine*, **39,** I58-I63.

Meehan, W. P., and R. G. Bachur, 2009: Sport-Related Concussion. *Pediatrics*, **123,** 114-123.

Prevost, T. P., A. Balakrishnan, S. Suresh, and S. Socrate, 2010: Constitutive response of brain tissue. *Acta Biomaterialia*, **to appear**.

Rudoy, D., S. Yuen, R. Howe, and P. J. Wolfe, 2010: Bayesian changepoint analysis with application to atomic force microscopy and soft material indentation. *Journal of the Royal Statistical Society Series C*, **to appear**.

Spagnoli, C., A. Beyder, S. R. Besch, and F. Sachs, 2007: Drift-free atomic force microscopy measurements of cell height and mechanical properties. *Review of Scientific Instruments*, **78**.

Suresh, S., 2007: Biomechanics and biophysics of cancer cells. *Acta Biomaterialia*, **3,** 413.

Taber, K. H., D. L. Warden, and R. A. Hurley, 2006: Blast-Related Traumatic Brain Injury: What Is Known? *J Neuropsychiatry Clin Neurosci*, **18,** 141-145.

Tanielian, T., and L. H. Jaycox, 2008: *Invisible Wounds of War: Psychological and Cognitive Injuries, Their Consequences,and Services to Assist Recovery*. RAND Corporation, 498 pp.

Van Vliet, K., G. Bao, and S. Suresh, 2003: The biomechanics toolbox: experimental approaches for living cells and biomolecules. *Acta Materialia*, **51,** 5881-5905.

Vanderploeg, R. D., G. Curtiss, C. A. Luis, and A. M. Salazar, 2007: Long-term morbidities following self-reported mild traumatic brain injury. *Journal of Clinical and Experimental Neuropsychology*, **29,** 585-598.

Yilmaz, S., and M. Pekdemir, 2007: An unusual primary blast injury - Traumatic brain injury due to primary blast injury. *American Journal of Emergency Medicine*, **25,** 97-98.